Water Research 229 (2023) 119468

Contents lists available at ScienceDirect

Water Research

journal homepage: www.elsevier.com/locate/watres

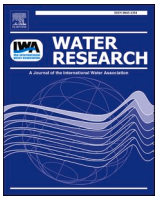

Agricultural nitrate export patterns shaped by crop rotation and tile drainage

Zewei Ma [a,b], Kaiyu Guan [a,b,c,*], Bin Peng [a,b,*], Murugesu Sivapalan [d,e], Li Li [f], Ming Pan [g], Wang Zhou [a,b], Richard Warner [h], Jingwen Zhang [a,b]

[a] Agroecosystem Sustainability Center, Institute for Sustainability, Energy, and Environment, University of Illinois at Urbana-Champaign, Urbana, IL 61801, USA
[b] Department of Natural Resources and Environmental Sciences, College of Agricultural, Consumer and Environmental Sciences, University of Illinois at Urbana-Champaign, Urbana, IL 61801, USA
[c] National Center for Supercomputing Applications, University of Illinois at Urbana-Champaign, Urbana, IL 61801, USA
[d] Department of Civil and Environmental Engineering, University of Illinois at Urbana-Champaign, Urbana, IL 61801, USA
[e] Department of Geography and Geographic Information Science, University of Illinois at Urbana-Champaign, Urbana, IL 61801, USA
[f] Department of Civil and Environmental Engineering, The Pennsylvania State University, University Park, PA 16802, USA
[g] Scripps Institution of Oceanography, University of California San Diego, La Jolla, CA 92037, USA
[h] National Great Rivers Research and Education Center, IL 62024, USA

ARTICLE INFO

Keywords:
Nitrate export
Water quality
Agricultural management
Hydrological mixing
Nutrient loss reduction, Modeling

ABSTRACT

Excessive agricultural nitrate export to aquatic systems degrades water quality and causes downstream ecological crises. Limited understanding of their underlying mechanisms and controls hinders mitigation measures. Here we analyzed observations of nitrate concentration (C) and discharge (Q) in 83 intensively managed agricultural watersheds across the central U.S. Midwest (37.0–44.5 N, 97.5–80.0 W), which reveals a regionally consistent pattern in C~Q relationships: C~Q relationship is chemodynamic at low flows and chemostatic at high flows, i.e., C increases with Q until a threshold beyond which C levels off. Motivated by this universal pattern, we developed a coupled model at the event scale that involves mixing of quick flow with high nitrate levels coming from shallow soils and the slow flow with low nitrate levels coming from deeper soils. Its implementation in combination with seasonal patterns of hydrology and agricultural practices explains observed patterns in the C~Q relationship across broad spatial and temporal scales and quantifies their main driving factors. Agricultural practices (i.e., corn fraction, nitrogen fertilizer use) explain 49% of spatial variability of C in quick flow during peak season, whereas tile drainage explains another 25%. Scenario analysis of changing area fraction of tile and corn using model projections sheds light on plausible pathways to assess and implement nutrient loss reduction goals.

1. Introduction

Aquatic pollution, for example, hypoxia zones and harmful algal blooms, is increasingly becoming a threat to water resources and human health. Excessive reactive nitrogen is one of the major factors leading to aquatic pollution (Howarth and Marino, 2006). Human activities are responsible for the increasing export of reactive nitrogen to aquatic systems over the past two centuries, and agricultural fertilizer is the main diffuse source of nitrogen pollution (Boesch, 2002; Galloway et al., 2004), especially in agricultural regions such as the U.S. Midwest. The expansion of agricultural fields (Zhang et al., 2015) and heavy use of synthetic fertilizers to boost crop yields (FAO, 2022) in the U.S. Midwest are increasing the input of nitrogen, introducing large doses of reactive nitrogen that ultimately spread across the entire Mississippi river basin and into the Gulf of Mexico, causing major environmental problems, including the formation of hypoxic zones (Rabalais et al., 2002), harmful algal blooms (Loftin et al., 2016), and degradation of water quality (Turner and Rabalais, 1994). Previous studies suggested that non-point pollution caused by agricultural management in the U.S. Midwest contributes to about 70% of nitrogen transported from the Mississippi River Basin to the Gulf of Mexico (Alexander et al., 2008; Robertson and Saad, 2021). Although state- and national-level nutrient loss reduction plans have been made for decades, there is still a lack of measurable progress in nutrient loss reduction at the regional and national scales (EPA, 2022;

* Corresponding authors.
E-mail addresses: zeweima2@illinois.edu (Z. Ma), kaiyug@illinois.edu (K. Guan), binpeng@illinois.edu (B. Peng).

https://doi.org/10.1016/j.watres.2022.119468
Received 28 May 2022; Received in revised form 28 November 2022; Accepted 4 December 2022
Available online 6 December 2022
0043-1354/Published by Elsevier Ltd.

NLRS, 2021). Understanding how nitrogen dynamics interact with hydrology in agricultural watersheds is critical to developing effective policies for the management of nutrient loss reduction (Bowles et al., 2018; Wollheim et al., 2018).

The relationship between solute concentration (C) and discharge (Q) has long been seen as an important signature of an integrated response to hydrological and biochemical processes in a watershed and has been used to understand the underlying mechanisms of solute transport (Godsey et al., 2009; Minaudo et al., 2019; Moatar et al., 2017; Musolff et al., 2015; Pohle et al., 2021). Generally, there are three kinds of C~Q relationships (Godsey et al., 2009). In the chemostatic relationship, C does not change with the change of Q, indicating a relatively homogeneous and uniform solute concentration distribution (Basu et al., 2010; Moatar et al., 2017). In the dilution pattern, C decreases with increasing Q, which manifests as a source-limited mechanism when the abundance of the solute limits its delivery to streams (Basu et al., 2011; Shanley et al., 2011). In the flushing pattern, C increases with increasing Q due to the flushing of solute. In this case, the transport capacity, rather than the abundance of solute, limits the solute delivery to the stream (Basu et al., 2011; Thomas et al., 2016).

Though a growing number of studies have studied the nitrate export patterns in the intensified agricultural landscapes through investigating the C~Q relationships (Marinos et al., 2020; Musolff et al., 2021), debates exist on the underlying mechanisms and the factors that drive variations in the C-Q relationship, especially at large spatio-temporal scales. A common perception is that nitrate export from agricultural lands typically follows chemostatic or stationary biogeochemical patterns (Basu et al., 2010; Bieroza et al., 2018; Gorski and Zimmer, 2021; Thompson et al., 2011). This posits that decades of agriculture fertilizer input has resulted in spatially-uniform legacy storage of soil N, such that inter-annual variations in total nitrogen export are small, leading to temporal invariance of the annual concentrations (Basu et al., 2010). However, recent meta-analyses have revealed that nitrate export patterns from agricultural lands instead mostly follow flushing patterns at a finer temporal resolution (e.g. biweekly and daily), meaning that nitrate concentration increases as discharge increases (Botter et al., 2020; Ebeling et al., 2021; Marinos et al., 2020; Zhi and Li, 2020). Multiple factors have been attributed to the observed nitrate export patterns. Specifically, Zhi and Li (2020) found that observed nitrate export patterns emerge from a switch between the dominance of shallow soil water at high streamflows and deeper groundwater at low streamflows, forming the so-called shallow and deep hypothesis. However, there is no consensus on which factors predominantly control nitrate variations and export patterns, and to what extent. As more extreme rainfall events are expected (Westra et al., 2014), understanding the event scale nitrate exporting mechanism is of great importance.

A distinct C~Q relationship has been recently reported in the U.S. Midwest region, a highly managed agricultural landscape: under relatively low Q conditions, the C~Q relationship exhibits a flushing pattern; under high Q conditions, a chemostatic C~Q relationship is observed (Koenig et al., 2017; Marinos et al., 2020). However, the underlying mechanisms remain elusive. Further, the spatial and temporal variation of meteorology and agricultural practices cause the spatial and temporal variabilities in hydrology and biogeochemistry, and how those variabilities regulate the nitrate C~Q relationship in this agricultural landscape is under-investigated. Temporally, agricultural practices change the seasonal field nitrogen balance. For example, synthetic nitrogen fertilizer increases soil nitrogen content in spring, and crop nitrogen uptake reduces field nitrogen content during the growing season. Besides, the runoff also shows a clear seasonal pattern. In spring, the high precipitation and snowmelt sustain the high river discharge (Baldwin and Lall, 1999). The temporal variation of hydrology and biogeochemistry has been shown to be a controlling factor in the temporal variation of the hypoxic region in the Gulf of Mexico (Bianchi et al., 2010; Laurent and Fennel, 2019). Spatially, the agricultural practices vary in different places. For example, the amount of synthetic fertilizer and tile drainage condition (density and efficiency) varies spatially (Cao et al., 2018; Nakagaki and Wieczorek, 2016). These different patterns of agricultural management factors over the landscape further result in the spatial heterogeneity of riverine nitrogen sources in the Mississippi River (David et al., 2010; Sinha et al., 2019). A systematic understanding of the spatial and temporal variation of the C~Q relationship and the underlying driving factors are therefore urgently needed to help identify "hot spots" and "hot moments" of nitrate export and to help further develop more effective and systematic nutrient loss reduction strategies over the broad Midwestern agricultural regions.

Here we systematically examined daily nitrate export patterns (concentration~discharge relationship, C~Q) in 83 intensively-managed watersheds of varying sizes in the central Midwest, across a large gradient of climate, geology, and land use conditions (e.g., corn area fraction and tile drainage percentage), and we found similar two-stage patterns in the studied watersheds (Fig. 1). The observation of this two-stage pattern led us to the overarching scientific questions: What are the underlying processes and causal factors that generate this unique and universal C~Q pattern in agriculture-dominated watersheds, and how do they regulate the spatial and temporal variation of C~Q patterns across different watersheds? Inspired by the "shallow and deep" hypothesis (Stewart et al., 2022; Zhi and Li, 2020), we hypothesized that the hydrological vertical mixing of quick flow from shallow soil and slow flow from deep soil directly shapes the distinct C~Q relationship observed in agricultural watersheds. We further hypothesized that the spatial and temporal variation of hydrology and agricultural management practices drive the spatial and temporal variation of the C~Q relationship.

The main goal of this study, thus, is to answer the above-mentioned scientific questions via testing two hypotheses. To accomplish the goal, we developed a hydrological vertical mixing model based on our hypotheses at both event and monthly scales. We further used the model to understand the spatial and temporal variation of the C~Q relationships and its underlying drivers. We finally parameterized the model and predicted the C~Q relationships in all the HUC8 watersheds over the central U.S. Midwest under different management scenarios, which can provide critical implications for designing effective nutrient loss reduction strategies.

2. Materials and methods

2.1. Study area and data

Our study area is the central U.S. Midwest, which is a heavily managed agricultural area. The majority of this region was once glaciated (Fig. 1), and rich glacier deposits were left behind, which later became the most fertile soil in the world (Huston, 2005). The glaciation also contributes to the poor drainage conditions in this region (Anders et al., 2018; Atkinson et al., 2014; Sears, 1926). The U.S. Midwest, which contributes up to ~30% of global corn and soybean production (FAO, 2022), has experienced extensive modification by human activities over the past 200 years, transforming from native prairies to uniform and highly productive agricultural landscapes (Fenneman and Johnson, 1946; Kalita et al., 2007). Extensive artificial tile drainage significantly improves drainage conditions and changes the dominant hydrological processes. Two major soil types in the region are Alfisols and Mollisols based on the USDA soil Taxonomy. Precipitation happens in all months and seasons and exhibits seasonal variation with more precipitation in the warm, summer seasons (Andresen et al., 2012; Baldwin and Lall, 1999).

We considered 83 stations (Fig. 1) in this region that had nitrate and discharge observations for more than 2 years. Among these sites, 61 are operated by the United States Geological Survey (U.S. Geological Survey, 2021), and the daily nitrate concentration and discharge data can be directly accessed via USGS API. 22 are operated by National Center for Water Quality Research (NCWQR) (Barbiero et al., 2018), and we

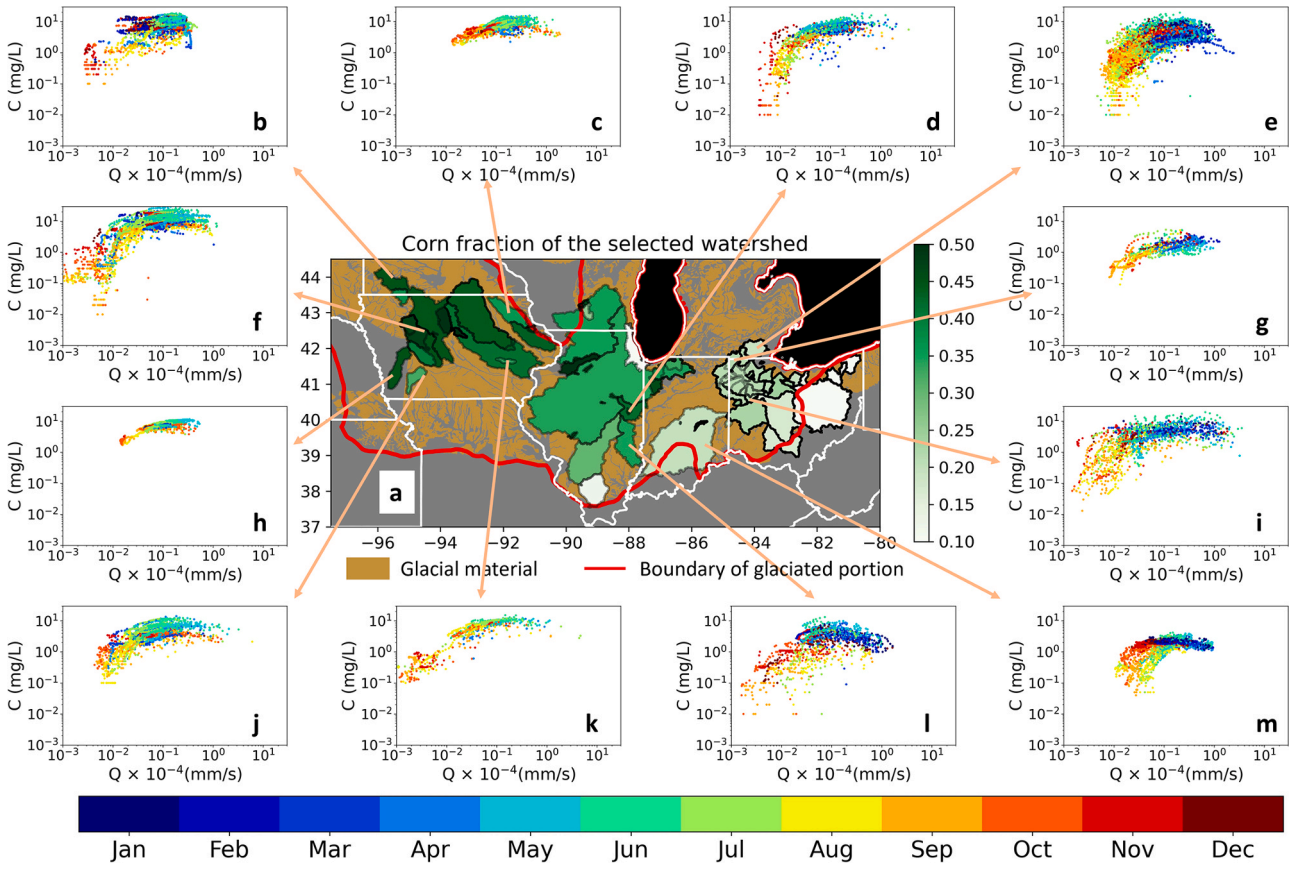

Fig. 1. Location of the study area and examples of nitrate concentration (C) ~ discharge (Q) relationships. a. Corn fraction of the selected watersheds in the central U.S. Midwest. The brown color represents the glacial material (Soller et al., 2009) and the red lines indicate the glaciated portion of the Central Lowland of the Interior Plains (Fenneman and Johnson, 1946). **b**. to **m**. Examples of the C~Q relationships in the central U.S. Midwest of selected watersheds. **b**. Des Moines River, IA; **c**. Turkey River, IA; **d**. Spoon River, IL; **e**. Raisin River, OH; **f**. North Raccoon River, IA; **g**. St Joseph River, IN; **h**. West Nishnabotna River, IA; **i**. Auglaize River, OH; **j**. Nodaway River, IA; **k**. Old Mans River, IA; **l**. Embarras River, IL; **m**. White River, IN.

calculated the daily flow weighted mean concentration based on multiple measurements on each day. Detailed information about data availability over each site can be found in Table S3. The upstream boundaries for each station were retrieved through USGS's NLDI web API (https://waterdata.usgs.gov/blog/nldi-intro/). The C~Q relationships in our study were plotted in the log-log space, and the discharge is normalized by the upstream drainage area. We calculated the corn/soybean area fraction, defined as the ratio of corn/soybean planting area to the total area of each watershed, based on the Cropland Data Layer (CDL, 2012–2020) from USDA NASS (NASS, USDA, 2021). The area fraction of tile drainage, defined as the ratio of tile-drained area to the total area of each watershed, is obtained from a USGS dataset (Nakagaki and Wieczorek, 2016). To support the regional prediction of the C~Q relationships and nitrate loading for all the HUC8 watersheds in the central U.S. Midwest, we used the daily discharge from the GRADES dataset, which is a well-calibrated and validated model-derived discharge database (Lin et al., 2019; Yang et al., 2019).

2.2. Methods

2.2.1. Hydrological vertical mixing model

A two-end-member mathematical model was developed to illustrate the mixing of quick flow and slow flow (Fig. 2) (Hooper et al., 1990). Total streamflow (Q) is the sum of quick flow (Q_{quick}) and slow flow (Q_{slow}), and the stream nitrate concentration (C) is then the weighted average of quick flow concentration (C_{quick}) and slow flow concentration (C_{slow}),

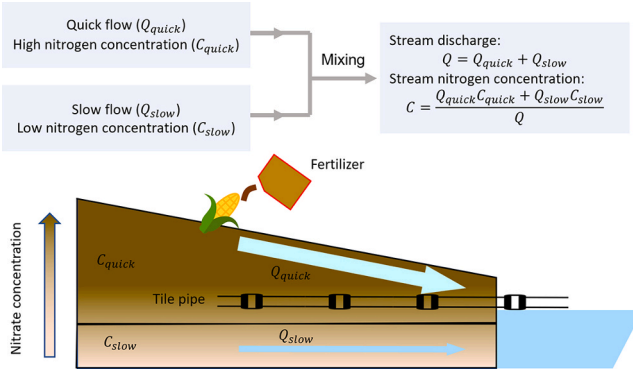

Fig. 2. Conceptual illustration of the hydrological vertical mixing model.

$$Q = Q_{quick} + Q_{slow} \tag{1}$$

$$C = \frac{C_{quick}Q_{quick} + C_{slow}Q_{slow}}{Q} \tag{2}$$

The nitrate concentrations of quick flow and slow flow exhibit distinct characteristics because of their distinctive flow pathways (Zhi and Li, 2020). Quick flow refers to runoff that follows flow pathways that respond quickly to rainfall events. The major sources of quick flow include surface flow, shallow subsurface flow, and tile drainage flow. The C in quick flow is generally high and also dynamic in agricultural

fields, due to the surficial nitrate input from nitrogen fertilization (Fig. 2). Slow flow refers to the flow pathways that respond slowly to rainfall events. The major sources of slow flow include deep subsurface water and groundwater, and the nitrate concentration in slow flow is generally low (Fig. 2).

2.2.2. Event-scale model development

The vertical mixing model was firstly applied at a single rainfall event. To detect the rainfall event, we firstly applied a 3-day moving average filter to the discharge time series. A valid rainfall event in our study was defined as those events with a recession length larger than 5 days. We assumed that Q_{slow} and C_{slow} remain constant during a rainfall event (Basu et al., 2012; Drury et al., 2016; Feldman, 2000; Hare, 2021; Lastoria, 2008; Li et al., 2020; Schilling et al., 2015; Van Meter et al., 2018). The dynamics of streamflow after a rainfall event were modeled via an exponential recession curve characterized with a recession rate k_1,

$$Q(t) = Q_0 e^{-k_1 t}, \tag{3}$$

where Q_0 is the initial streamflow during a rainfall event [mm/s], and k_1 is the flow recession rate [1/day]. t is the number of days after the occurrence of a rainfall event [days]. Then, Q_{quick} is the difference between Q and Q_{slow},

$$Q_{quick} = Q - Q_{slow} \tag{4}$$

As there is no explicit equation describing the dynamics of nitrogen concentration in soil/stream after a rainfall event, we assumed for simplicity C_{quick} changes linearly after a rainfall event,

$$C_{quick} = C_{quick0} - k_2 t, \tag{5}$$

where C_{quick0} is the initial quick flow concentration during a recession process [mg/L], and k_2 is the change rate of the quick flow concentration [mg/L/day]. The model sensitivity suggested that the C~Q relationship is not sensitive to k_2 (Fig. S21). Integrating equation (1–5), we obtained the expression of C in a rainfall event (see details in Supplementary),

$$C = \frac{C_{slow}Q_{slow} - \left(C_{quick0} + \frac{k_2}{k_1} ln\ \frac{Q_0 - Q_{slow}}{Q - Q_{slow}}\right)Q_{slow}}{Q} + \left(C_{quick0} + \frac{k_2}{k_1} ln\ \frac{Q_0 - Q_{slow}}{Q - Q_{slow}}\right) \tag{6}$$

2.2.3. Monthly-scale model development

To investigate how the seasonal variation of biogeochemical factors and hydrological factors drive the seasonal variability of the C~Q relationship, we further applied the hydrological vertical model at the monthly scale. We first constructed a conceptual equivalent rainfall event for each month with the monthly statistics derived from historical hydrography and observed stream nitrate concentrations. The conceptualized rainfall event statistically characterizes the flow recession process and nitrogen dynamics separately in different months (Fig. 3). The maximum discharge (Q_{max}) and minimum discharge (Q_{min}) of a conceptualized rainfall event are defined as the 95th percentile discharge (Q_{95}) and 5th percentile discharge (Q_{05}) in a certain month from multi-year observations, respectively.

To estimate slow flow, a digital filter was applied to the daily discharge time series to separate water flow into two parts, the quickly responding part (Q_{qr}) and the slowly responding part (Q_{sr}). In this study, the digital filter method by Lyne and Hollick (1979) was applied. Then, the slow flow in a certain month (Q_{slow}) was then defined as the average Q_{sr} in this month. An additional upper-bound constraint was applied here to make sure the model is both physically and numerically correct,

$$Q_{slow} = min\{mean\{Q_{sr}[t \in month]\},\ Q_{05}\} \tag{7}$$

The initial quick flow (Q_{quick0}) was then defined as the difference between Q_{max} and Q_{slow},

$$Q_{quick0} = Q_{max} - Q_{slow} \tag{8}$$

To estimate the flow recession rate of the monthly conceptualized rainfall event, we first extracted all rainfall events in a certain month (Fig. 3). Then, the flow recession rate in the monthly conceptualized rainfall event (k_1) was estimated using the averaged $k_{1,\ event}$ for single rainfall events happening in a certain month,

$$k_1 = mean\{k_{1,\ event}\} \tag{9}$$

We here estimated the C_{quick} using the average nitrate concentration between the 90th percentile of discharge (Q_{90}) and 95th percentile discharge (Q_{95}) in a certain month from multi-year observations, and C_{quick} defined here was used as the initial quick flow concentration in the conceptualized rainfall event,

$$C_{quick0} = C_{quick} = mean\{C[Q \in [Q_{90}, Q_{95}]]\} \tag{10}$$

The change rate of quick flow concentration k_2 was defined with the gradient of C_{quick0},

$$k_2 = \nabla C_{quick0} \tag{11}$$

In this study, we categorized the dynamics of quick flow concentration into four periods in the hydrology year: 1) The dormant period (from November to March), in which the low-temperature limits microbial activity, and nitrate concentration has little change. 2) The fertilization period (from March to June), during which the use of synthetic fertilizer increases the soil nitrate concentration. 3) The plant

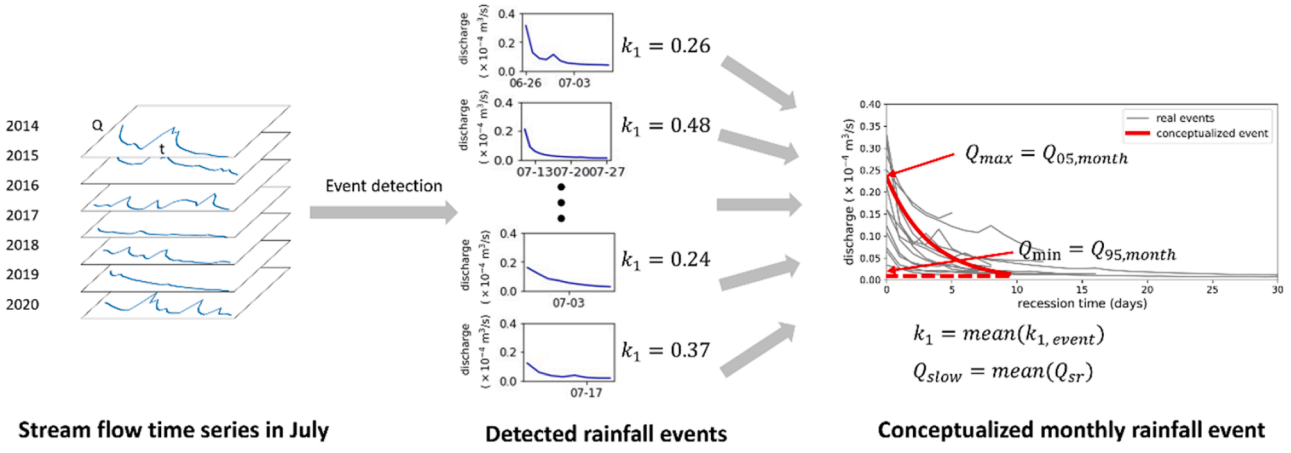

Fig. 3. Flow chart for constructing the monthly conceptualized rainfall event.

uptake period (from June to August), during which plant uptake is the major process that consumes soil nitrate and reduces the stream nitrate concentration. 4) The mineralization period (from August to November), during which the mineralization of crop residue increases the soil nitrate concentration. During the fertilization and mineralization periods, k_2 is negative. During the plant uptake period, k_2 is positive.

C_{slow} was estimated by the average nitrate concentration of the flow with the lowest 5th percentile discharge from all observations,

$$C_{slow} = const = mean\{C[Q \le Q_{05,\ all}]\} \tag{11}$$

By substituting the above parameters in Eq. (6) with the parameters in the monthly conceptualized rainfall event, we could get the monthly concentration model (see details in Supplementary).

2.2.4. Model sensitivity, parameterization, and validation

To further understand the spatial variation of the C~Q relationships, we examined the relationship between watershed characteristics (i.e. corn fraction and tile fraction) and the parameters (i.e. Q_{min}, Q_{max}, C_{quick0}, C_{slow}, Q_{slow}) that determine the shape of the watershed C~Q relationship in the monthly hydrological vertical mixing model. To extend the C~Q relationship to a broader scale, we further established empirical relationships between the watershed characteristics (i.e. corn fraction and tile fraction) and nitrate concentration parameters (i.e. C_{quick} and C_{slow}) in the monthly hydrological vertical mixing model. Based on the nature of nitrate dynamics, we made three assumptions: (1) C_{slow} was constant for the whole year; (2) C_{quick} was dynamic all over the year, and the dynamics of C_{quick} were characterized into four periods in a hydrology year (i.e. the dormant period, the fertilization period, the plant uptake period, and the mineralization period, as defined in Section 2.2.3); (3) C_{quick} changed linearly within each period. We first established empirical relationships to estimate C_{slow} and C_{quick} in June, August, and November,

$$C_{quick,\ Jun} = 0.15 * e^{8.16 * CornFraction} + 8.88 * TileFraction \tag{12}$$

$$C_{quick,\ Aug} = 1.28 * e^{3.21 * CornFraction} - 0.61 * (SoybeanFraction + CornFraction) \tag{13}$$

$$C_{quick,\ Nov} = 0.73 * e^{4.17 * CornFraction} + 7.80 * SoybeanFraction \tag{14}$$

$$C_{slow} = 4.52 * e^{-3.58 * TileFraction} \tag{15}$$

C_{quick} in other months were interpolated following our assumptions (see details in Supplementary). The estimation of C_{quick} and C_{slow} were then validated using the leave-one-watershed-out cross-validation method.

To better understand the importance of corn fraction and tile fraction in nitrate export, we then attributed the spatial variation of C_{quick} to the spatial variation of corn fraction and tile fraction in June, the month with the highest nitrate concentration in all studied watersheds, following:

$$var(a+b) = var(a) + 2Cov(a,b) + var(b) + ErrorTerm \tag{16}$$

where a is the corn fraction related term ($0.15 * e^{8.16 * CornFraction}$), and b is the term related to tile fraction ($8.88 * TileFraction$) in equation (12).

We validated our hydrological mixing model and parameterization at different levels. First, we compared the observed nitrate concentration with the following predictions: (1) predicted nitrate concentration estimated with the event-scale hydrological vertical mixing model, (2) predicted nitrate concentration estimated with the monthly-scale hydrological vertical mixing model without parameterization, (3) predicted nitrate concentration estimated with the monthly-scale hydrological vertical mixing model with parameterization in all 83 watersheds. Three statistical criteria were used to indicate model performance, Pearson correlation coefficient (r), root mean square error (RMSE), and bias.

We further evaluated the performance of monthly nitrate loading estimation by comparing the nitrogen loading estimated via the monthly scale hydrological vertical mixing model with observations at all 61 USGS gauges. In the hydrological vertical mixing model estimation, the nitrate concentration was firstly estimated with the developed monthly C~Q relationship based on the observed discharge, i.e. $C = f(Q)$. The flow ranges from 5th percentile discharge (Q_{05}) to 95th percentile discharge (Q_{95}) in a monthly conceptualized rainfall event. Here, we assumed that the nitrate concentration for discharges smaller than the 5th percentile discharge is $f(Q_{05})$ and the nitrate concentration for discharges larger than the 95th percentile discharge is $f(Q_{95})$. The nitrate loading (L) is then the product of discharge and concentration, i.e. $L = CQ$. Similarly, the observed nitrate loading was estimated as the product of observed discharge and nitrate concentration at the USGS gauges. To gap fill and estimate daily nitrate concentrations, we used the state-of-the-art and most widely used the Weighted Regressions on Time, Discharge, and Season (WRTDS) method, which is a regression model that uses time, discharge, and seasons as explanatory variables as predictors of nitrate concentrations (Hirsch et al., 2010; Hirsch and De Cicco, 2015),

$$ln(C) = \beta_0 + \beta_1 t + \beta_2 ln(Q) + \beta_3 sin(2\pi t) + \beta_4 cos(2\pi t) + \varepsilon \tag{17}$$

where t is time in decimal years, C is the daily concentration, Q is daily discharge, $\beta_0 \sim \beta_4$ are fitted coefficients, and ε is the error term.

2.2.5. Scenario analysis

Increased spring wetting has been projected for the U.S. Midwest (Pachauri et al., 2014), which may lead to increasing adoption of tile drainage to improve soil drainage conditions (NASS, USDA, 2019a). Besides, recent years have seen the trend of expansion in corn planting acreage due to increased needs for grain and bioenergy production (Cheng et al., 2022; Foley et al., 2011), as well as an overall heavier use in nitrogen fertilizer (Cao et al., 2018) (though the trend has been slowed down due to the high fertilizer cost recently). To understand how the change of tile drainage fraction and corn fraction affects nitrogen exporting, we used the developed C~Q relationship model to calculate nitrate loading in June, one of the months with the highest nitrogen loading, in two major scenarios: (1) increase tile fraction by 10%, 20%, 30% (e.g. tile fraction increases from 40% to 44%, 48%, and 52%, respectively), and (2) increase/decrease corn fraction by 20% (e.g. corn fraction increases/decreases from 40% to 48% and 32%, respectively), over all the HUC8 watersheds in the central U.S. Midwest, to examine how the change of tile drainage and corn fraction would change the nitrate loading in June. In each scenario, we first predicted the C~Q relationships based on the corn fraction and tile fraction and the GRADES dataset. We then calculated the nitrate loading in June for each scenario with the predicted C-Q relationships. The predicted nitrate loading was then averaged from 1980 to 2013 for comparison among different scenarios.

3. Results

3.1. Model validation results

3.1.1. Validation of nitrate concentration estimation

The developed hydrological vertical mixing model revealed a satisfactory performance in nitrate concentration estimation. Over the 83 watersheds in the studied area, the Pearson correlation coefficient (r), RMSE, and bias are 0.84, 2.23 mg/L, −0.04 mg/L for the event-scale hydrological vertical mixing model, 0.76, 2.51 mg/L, −0.43 mg/L for the monthly-scale hydrological vertical mixing model without parameterization, and 0.66, 2.96 mg/L, −0.70 mg/L for the monthly-scale hydrological vertical mixing model with parameterization, respectively

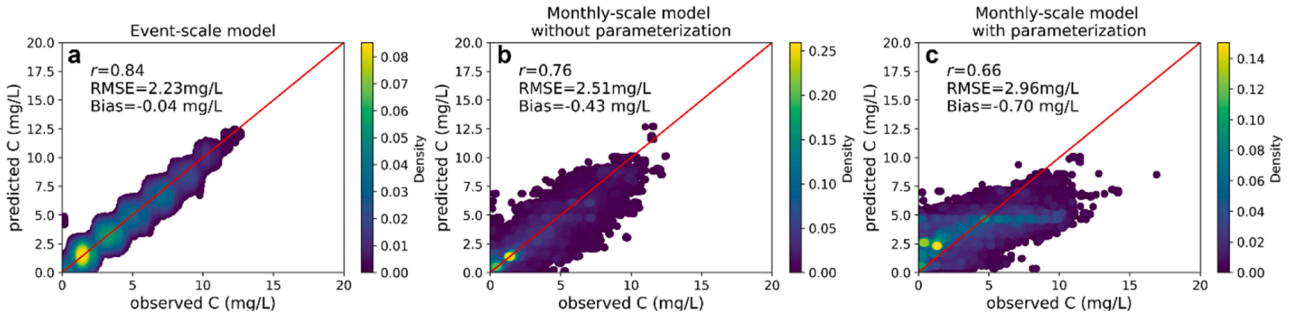

Fig. 4. Validation of daily nitrate concentration (C) estimation for all 83 watersheds for **a**. event-scale hydrological vertical mixing model, **b**. monthly hydrological vertical mixing model without parameterization of C_{quick} and C_{slow}, and **c**. monthly hydrological vertical mixing model with parameterization of C_{quick} and C_{slow}. The density is the normalized bi-dimensional histogram of the observed and simulated daily nitrate concentration.

(Fig. 4). The high r and low RMSE show the ability to use the hydrological vertical mixing model to further understand the spatial and temporal variability of the C~Q relationships. The decrease of r and increase of RMSE and bias from event-scale hydrological vertical mixing model to monthly-scale hydrological vertical mixing with parameterization indicates that the model uncertainty accumulates as we increase the complexity of the model when introducing conceptualized monthly rainfall event and parameterization.

3.1.2. *Validation of C_{quick} and C_{slow} parameterization*

Fig. 5, Table S1, and Fig. S9 show the results of leave-one-watershed-out cross-validation of estimating nitrate concentration parameters (i.e. C_{quick} and C_{slow}) using parameterization with corn and tile fractions. The overall *r*, RMSE, and bias for the C_{quick} estimation are 0.70, 2.48 mg/L, and −0.14 mg/L, respectively. The *r*, RMSE, bias for C_{quick} estimation in each month range from 0.45 to 0.77, from 1.55 mg/L to 3.25 mg/L, and from −0.61 mg/L to 0.40 mg/L, respectively. The C_{quick} estimation performs better in the spring (r>0.70), when there is less human perturbation. The C_{quick} estimation performs worse in the fall (r<0.65), and r is lowest in October when harvesting happens (r=0.45). The performance of estimating C_{slow} is relatively lower than C_{quick} with overall *r*, RMSE and bias of 0.50, 1.70 mg/L, and −0.14 mg/L, respectively. These results support that the empirical relationships developed here could be used to predict the C~Q relationships in ungauged watersheds at different months.

3.1.3. *Validation of monthly nitrogen loading estimation*

We further compared the predicted monthly nitrogen loading with observations from 61 USGS gauges (Fig. 6). The *r* between monthly nitrogen loading estimated via our hydrological mixing model and that estimated by the WRTDS method is 0.96, and the corresponding RMSE, and bias are 0.04 g/m^2, and 0.00 g/m^2, respectively (Fig. 6), which demonstrates that our model has high accuracy in predicting monthly nitrate loading.

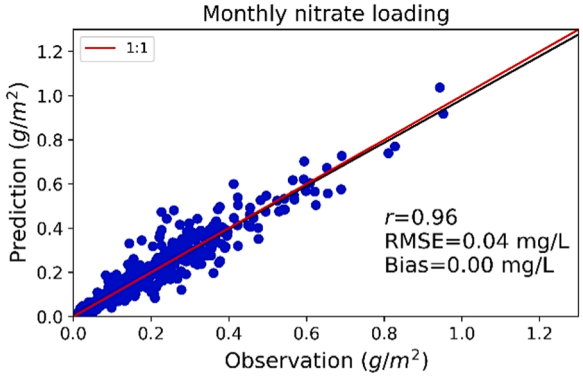

Fig. 6. Validation of the monthly nitrate loading at the USGS gauges. Monthly nitrate loading was aggregated from the daily nitrate loading. Daily nitrate loading was calculated as the product of daily discharge and daily nitrate concentration. Observation is the monthly nitrate loading calculated with WRTDS gap-filled USGS nitrate concentration observations. Prediction is the monthly nitrate loading calculated with the nitrate concentration estimated with our monthly hydrological vertical mixing model without parameterization.

3.2. *Hydrological vertical mixing on the C~Q relationship*

The C~Q relationships from modeling and observation were compared, and both the event-scale and the monthly-scale hydrological mixing model were found to be able to well reproduce the observed C~Q relationships at the watershed scale (Figs. 7 and S10). Fig. 7 is an example of the monthly C~Q relationships in the Spoon River watershed, IL from May 22, 2013 to June 13, 2021. The "two-stage" shape

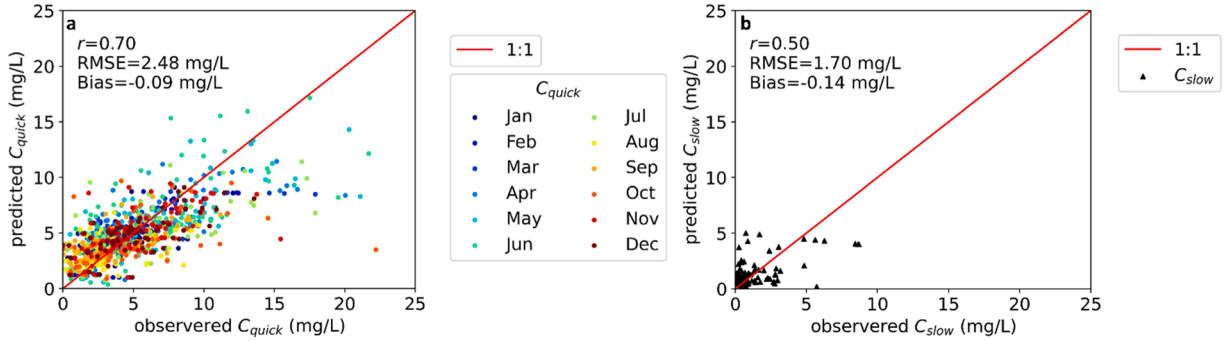

Fig. 5. Leave-one-watershed-out validation of nitrate concentration parameterization in the monthly-scale hydrological vertical mixing model. a. leave-one-watershed-out validation for C_{quick}. **b**. leave-one-watershed-out validation for C_{slow}.

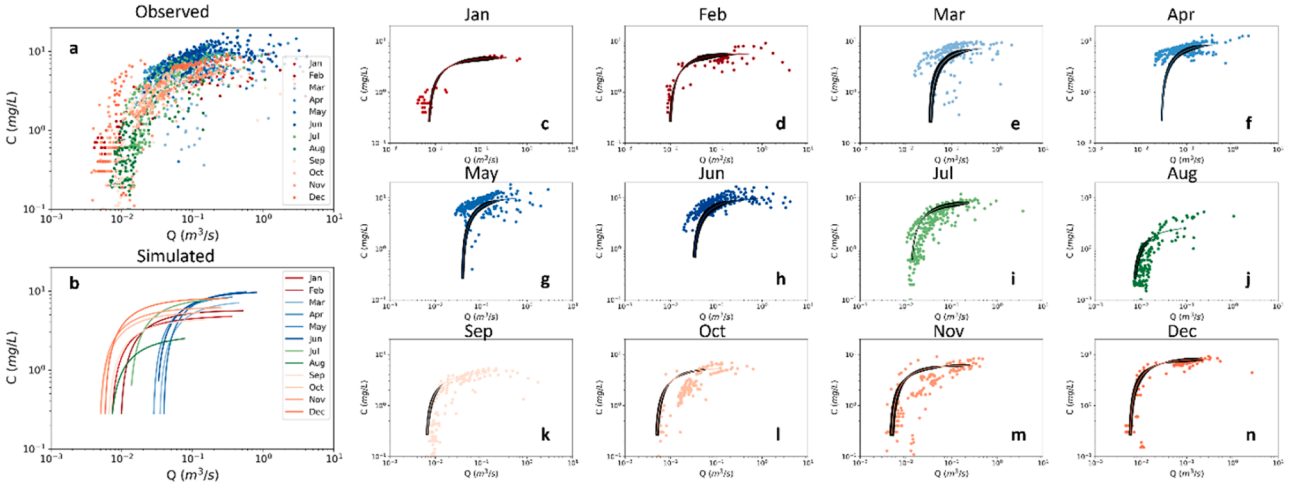

Fig. 7. The observed and simulated nitrate concentration (C) ~ discharge (Q) relationships in the Spoon River watershed in central Illinois from May 22, 2013 to June 13, 2021. a. The observed C~Q relationships. **b**. The simulated C~Q relationships. **c**. to **l**. The C~Q relationship from January to December. The thickness of lines in **c**. to **l**. represents the density of streamflow distribution, details can be found in Fig. S11.

agrees well with the observed data, which shows that C increases with the increase of Q at low flow conditions and then levels off at high flow conditions. Further, the monthly-scale hydrological vertical mixing model successfully reveals the seasonal dynamics of the C~Q relationship. The nitrate concentration at high flow conditions is highest from March to June, and it decreases gradually from July to August, which moves the C~Q relationship downwards along the y-axis. From September to November, the nitrate concentration at high flow conditions increases, which moves the C~Q relationship upwards along the y-axis. Besides, the distributions of the streamflow peak at the high flow regions from March to June, suggesting that the quick flow dominated the C~Q relationship regime during this period (Figs. 7 and S11). The streamflow distribution in July is more positively skewed, and the discharge peaks at a smaller value compare to the distribution in June, indicating a drier condition. The streamflow distribution in August, with only one peak in the low flow region, indicates that slow flow is one of the controlling factors in that month. The streamflow distributions from September to February have two or more peaks, with at least one in slow flow regions and one in high flow regions, which shows a transition from the slow flow dominated regime to the quick flow dominated regime in those months (Figs. 7 and S11).

3.3. *Sensitivity of the monthly-scale hydrological model to corn and tile fractions*

The correlations between watershed characteristics (corn and tile fractions) and parameters in the monthly hydrological vertical mixing model in June are shown in Table 1. We found that the planting of corn changes the hydrological and biogeochemical processes, especially, C_{quick} and Q_{slow}, and further controls the C~Q relationship at the watershed scale. C_{quick} shows a significant positive relationship ($r = 0.54$ and $p < 0.001$) and increases exponentially with increasing corn fraction (Fig. S12), indicating that a large portion of stream nitrate originates from fertilizer application in cornfields (Donner et al., 2004; Kohl et al., 1971). Q_{slow} in June also significantly correlates with corn fraction ($r = 0.47$ and $p < 0.001$). Evapotranspiration (ET) of croplands is low in May and June compared to that in forests and grassland (Liu et al., 2016; Mishra et al., 2010), and the relatively low ET leads to more water storage in June, which explains why Q_{slow} in June is higher in the watersheds with higher corn fraction. Other critical variables of the C~Q relationship (e.g. Q_{min}, C_{max}, and C_{slow}) either have no significant correlation or weak correlation with corn fraction (Fig. S12 and Table 1). Based on these empirical results, we established statistical models between corn fraction and the parameters that showed statistically significant relationships ($p < 0.05$, C_{quick}, Q_{min}, Q_{max}, and Q_{slow}). Integrating these relationships with the hydrological vertical mixing model, we found that increasing corn fraction moves the C~Q relationship towards the top right corner (Fig. 8). When corn fraction is 10% or lower, nitrate concentration remains relatively stable with the change of streamflow, indicating that the observed distinct "two-stage" C~Q relationship might be a unique feature in the agricultural landscapes, which is very different from the C~Q relationships found in forests and urban regions (Zhi and Li, 2020).

We also found significant correlations between tile fraction and parameters in the hydrological vertical mixing model (Table 1), which confirms that tile drainage modifies hydrological processes and further influences the biogeochemical cycle in the agroecosystems. In June, C_{quick} is significantly correlated with tile fraction across all watersheds, and C_{quick} is higher in watersheds with more tile-drained fields (Fig. S13, $r = 0.36$, $p < 0.001$). This relationship can be explained largely by decreasing residence time and less nitrogen absorption by the soil in tile-drained fields (Schilling et al., 2015). C_{slow} decreases exponentially with increased tile fraction (Fig. S13, $r = -0.44$), suggesting that tile drainage reduces the contribution of water above tile drainages to slow flow, and increases the relative contribution of water from deeper soil with lower nitrate concentration contributing to slow flow. We also found that Q_{max} in June has a positive correlation with tile drainage fraction (Fig. S13, $r = 0.45$ and $p < 0.001$), and Q_{slow} and C_{slow} in June are negatively correlated with tile fraction, also suggesting that tile drainage facilitates quick flow drainage and reduces water penetration that contributes to deeper, slower flow (Fig. S13, $r = -0.30$ for Q_{slow}, Fig. S13, $r = -0.44$ for C_{slow}). Increasing tile fractions, therefore, moves the C~Q relationship toward the top left corner (Fig. 8). When tile fraction is only 10%, the C~Q relationship tends to be chemostatic, indicating that tile drainage is a contributing factor to the distinct "two-stage" C~Q relationship in these agriculture-dominated watersheds.

Table 1
Pearson correlation coefficient (*r*) between monthly C~Q relationship model parameters and watershed characteristics (Corn Fraction and Tile Fraction) (*** $p < 0.001$; ** $p < 0.01$; * $p < 0.05$, p-value was corrected with Holm-Bonferroni method to control type one errors).

	$C_{quick,\ Jun}$	$Q_{min,\ Jun}$	$Q_{max,Jun}$	Q_{slow}	C_{slow}
Corn Fraction	0.54 ***	0.28 *	−0.24 *	0.47 ***	0.21
Tile Fraction	0.36 ***	−0.42 ***	0.45 ***	−0.30 **	0.44 ***

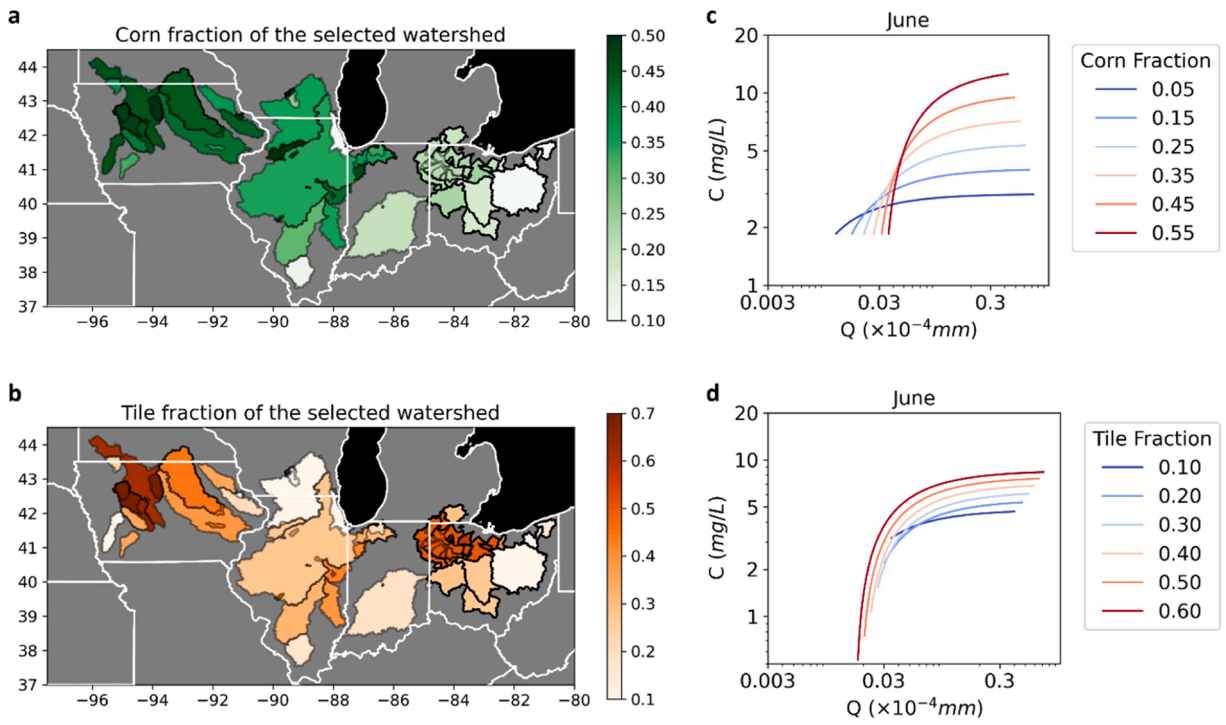

Fig. 8. The responses of nitrate concentration (C) ~ discharge (Q) relationship to tile fraction and corn fraction. a. Corn fraction of the selected watersheds. **b.** Tile fraction of the selected watersheds. **c.** The response of the C~Q relationship to corn fraction. **d.** The response of the C~Q relationship to tile fraction.

3.4. Nitrate concentration prediction at all HUC8 watersheds in the central U.S Midwest

We further predicted the monthly C_{quick} at all HUC8 watersheds in the central U.S. Midwest (Fig. 9). The results show that watersheds in Iowa, central Illinois, central Indiana, and central Ohio have the highest C_{quick} (Fig. 9), and those watersheds have the highest corn fraction or tile fraction (Fig. S15). The spatial pattern of the predicted C_{quick} is largely consistent with the riverine nitrate yield pattern estimated by David et al. (2010), suggesting that high flow carries the majority of the nitrate loading. Further, the results also reveal the temporal variation of C_{quick}, i.e. C_{quick} decreases from June to August, and then increases from August to November (Figs. S9 and S16).

3.5. Scenarios of nitrate export

Our HUC8-level C~Q relationship model predicts that an increase of tile drainage fraction would increase nitrate loading for all the HUC8 watersheds in the central US Midwest (Fig. 10a-c). This is especially the case in northeast Indiana and northern Ohio, where a 30% relative increase of tile fraction under current conditions would lead to 20% more nitrate loading in June (Fig. 10c). Larger nitrate loading occurs in watersheds with high tile drainage fractions, highlighting the importance of tile drainage in nitrate leaching management.

The model also predicted diverse nitrate loading under the scenarios of increasing or decreasing "corn fraction" by 20% (Fig. 10d-e). Interpreting this result requires more caution, as here we did not explicitly account for nitrogen fertilizer use information at the watershed scale due to lack of such information. Changing "corn fraction" here means the combined effects of changing corn acreage and changing nitrogen fertilizer usage. We found that both increase and decrease of "corn fraction" result in a great amount of nitrate loading change, especially in watersheds that currently have high corn fraction. A 20% relative increase of "corn fraction" under current conditions could lead to a considerable increase in nitrate loading in June. For example, nitrate loading would increase by more than 50% in the northwest watershed in Iowa (Fig. 10d). On the contrary, the reduction of "corn fraction" effectively reduces the nitrate loading in June (Fig. 10e). These alarming results highlight opportunities for making significant progress by managing our landscape through crop rotation and nutrient management. Although we generally know that high corn fractions would lead to a high nitrogen fertilizer amount and thus a high nitrate loading, results here show that nitrate loading increases exponentially with corn fraction, possibly because farmers tend to devote more fertile land and apply more fertilizer in growing corn (EPA, Illinois, 2021). Differentiating the effects of corn planting acreage and fertilizer application is necessary for designing effective nutrient loss reduction strategies.

4. Discussion

4.1. On the effectiveness of the hydrological vertical mixing model

Our results show that the hydrological vertical mixing is able to reproduce the C~Q relationship and predict C via a two-end-member mixing model. The spatial distribution of solute content in the watershed has long been seen as a controlling factor in nutrient export (N.B. Basu et al., 2011; Zhi and Li, 2020). In particular, Zhi and Li (2020) found that the "shallow and deep" hypothesis successfully explained the signatures of the C~Q relationship in watersheds with different land cover types (i.e. urban, agriculture, and undeveloped). Our hydrological vertical mixing model further extended this hypothesis, and successfully explained the distinct "two-stage" nitrate C~Q relationship in the agricultural watershed in the central U.S. Midwest (Figs. 7 and S9). In agricultural watersheds, synthetic nitrogen fertilizer is the dominant nitrate source, and the use of nitrogen fertilizer lifts the soil nitrogen content, especially in the shallow soil columns, which further leads to a stratified nitrogen vertical profile (e.g. Hahne et al., 1977; Van Meter et al., 2016). Quick flow (i.e. surface runoff, interflow, and tile flow) from shallow soil with high nitrate concentrations is the major source of nitrate in streamflow after precipitation. With the decrease of streamflow, the stream nitrate concentration decreases as the contribution of slow flow from deeper soil with low nitrate concentration increases.

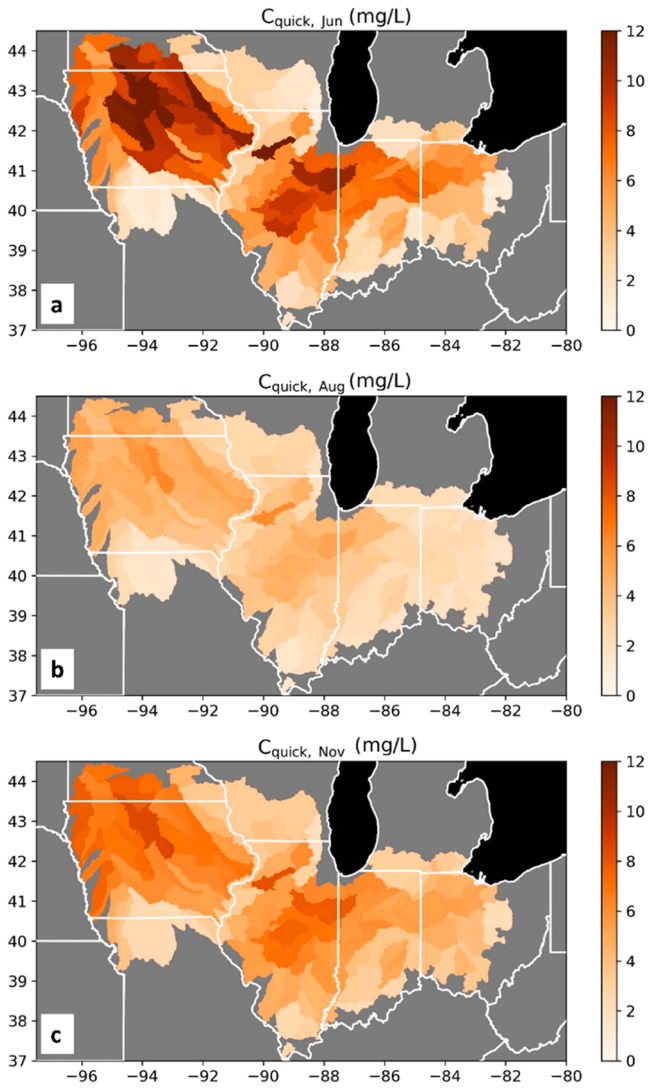

Fig. 9. Predicted C_{quick} at all HUC8 watersheds in the central U.S. Midwest for **a**. June, **b**. August, and **c**. November.

The hydrological status (i.e. soil moisture condition) determines the runoff generation process and further affects the C~Q relationship. In the wet period (March to June), the high precipitation and low plant water uptake lead to high soil moisture, and the water from shallow soil is the major stream water source. Therefore, the C~Q relationship is dominated by quick flow, and is more stationary mainly spanning the high flow region during the wet period (Fig. 7) (Winter et al., 2022). In the dry periods, either low precipitation or high water uptake by crops results in low soil moisture, and groundwater from deeper soil is the major source of streamflow (Winter et al., 2022). The C~Q relationship exhibits a transition from the quick-flow-dominated regime to the slow-flow-dominated regime during a rainfall event (Fig. 7), and exhibits a flushing pattern in this period.

The model uncertainty gradually increases with the increase of model complexity (Fig. 4). In the event-scale hydrological mixing model, the two-end-member mixing model is a reasonable simplification of real mixing processes. However, a two-end-member mixing model could not capture the dilution pattern during flooding, during which a large amount of surface water with low nitrate concentration directly flows into the stream from precipitation (e.g. Fig. 1e and 1i). Besides, the complexity and heterogeneity properties of the watersheds might require models with more end members to capture the dynamics of nutrients (Lee and Krothe, 2001; Saiers et al., 2021). All those factors contribute to the uncertainty of the two-end-member hydrological vertical mixing model. From the event-scale model to the monthly-scale model, the use of conceptualized rainfall events ignores the intra-annual variabilities of hydrological and biogeochemical processes, which further increases the model uncertainty. Finally, model parameterization further increases the model uncertainty since the parameterization did not consider all information about watershed characteristics. Specifically, nitrate export patterns are different under different land cover types (i.e. urban area, agriculture area, and forest area) (Musolff et al., 2021; Zhi et al., 2021). Further, the complex spatial organization of different landscapes within the watersheds might also change the nitrate export pattern (e.g. Figs. S4-S8; Hansen et al., 2018), which is not considered here. Compared with C_{quick}, the parameterization of C_{slow} exhibits higher uncertainty (Fig. 5). We hypothesized that the stream denitrification accounts for the high uncertainty of C_{slow}. Existing studies have shown that stream denitrification plays a more important role under low flow conditions to remove stream nitrogen, with shallower stream water depth and smaller flow velocity (N.B. Basu et al., 2011; Böhlke et al., 2009). Different controlling factors of stream denitrification (e.g. organic substrate, river bedforms, drainage density, etc.) showing large spatial heterogeneity might increase the parameterization uncertainty of C_{slow} (Gomez-Velez et al., 2015; Harvey et al., 2013; Inwood et al., 2007; Mulholland et al., 2008; Pinay et al., 2000).

4.2. *The impact of agricultural practices on nitrate export*

Corn fraction has been shown to be the leading factor that drives the spatial variation of nitrate export pattern, mainly through the biogeochemical cycle. Corn fields are the major consumers of synthetic fertilizer nitrogen in the U.S. Midwest (NASS, USDA, 2019b), which increases nitrate concentration in streams. Specifically, the spatial variation of corn fraction has been found to explain half of the spatial variability of C_{quick} in June, and the change of corn fraction in our hypothetical scenario analysis also highlights the importance of corn fraction and fertilizer application for nutrient loss reduction.

We found that the seasonal variation of C_{quick} largely follows the temporal pattern of field-level farmland nitrogen dynamics in the shallow soil layer when averaged over the 83 watersheds in the U.S. Midwest (Fig. 11). In particular, C_{quick} increases from March to June (Fig. 11), corresponding to synthetic fertilizer application for corn (Cao et al., 2018) and increased soil mineralization during the wet and warming-up period during spring and early summer, both of which elevate soil inorganic nitrogen (SIN). The C_{quick} then decreases from June to August, primarily due to plant uptake of SIN. From September to November, C_{quick} slowly increases due to the mineralization of soil organic nitrogen in Fall, especially in soybean fields (King et al., 2016). With generally low microbial activities at low temperature from November to February, C_{quick} remains relatively stable. These watershed-scale patterns closely mimic SIN dynamics measured and simulated over several farmlands (Archontoulis et al., 2020; Martinez-Feria et al., 2018), indicating the aggregated field-level SIN dynamics largely control the watershed nitrate export behavior.

Our results show that corn fraction significantly correlates with C_{quick} in all twelve months, indicating strong control of corn planting on C_{quick} (Fig. S17, r: 0.40–070, $p < 0.001$). This pattern may arise from both short-term and long-term legacy effects of hydrology and biogeochemical cycles arising from agricultural practices. Growing more corn with high fertilizer application generally leads to a relatively higher level of nitrate storage in agricultural lands and export to rivers and streams. Longer residence time of groundwater and absorption of nitrate in soils can delay nitrate export to streams (Van Meter et al., 2016). Crop and soil microbes can uptake inorganic nitrogen in fertilizer and return nitrogen back to the soil later in the form of organic nitrogen such as plant residue (Quan et al., 2021). The decomposition of organic nitrogen in plant residue, which happens at any time, also contributes to nitrate

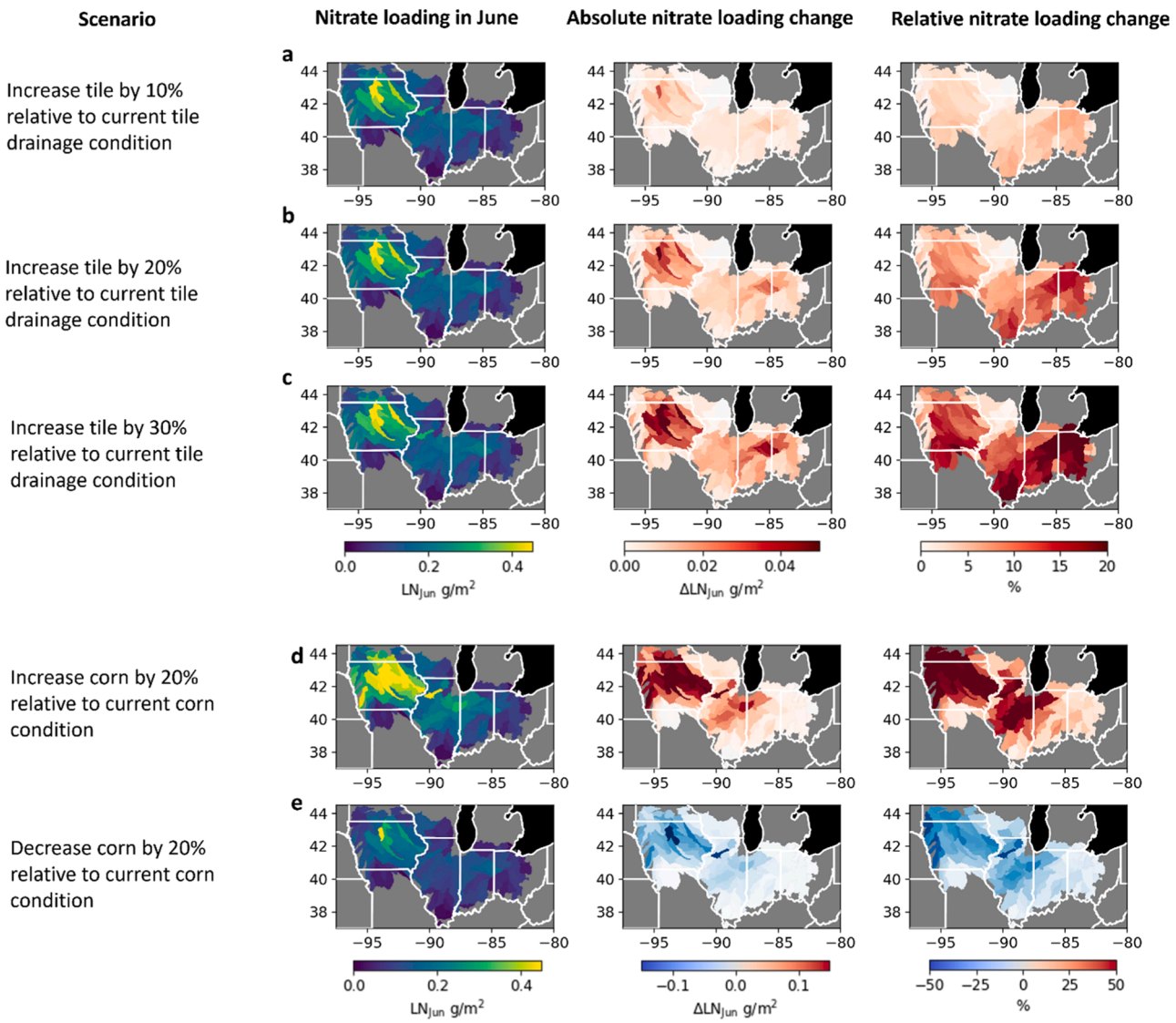

Fig. 10. Scenario analysis of nitrate loading. Nitrate loading (LN), its absolute and relative changes under the cases of **a.** increase 10% tile, **b.** increase 20% tile, **c.** increase 30% tile, **d.** increase 20% corn, and **e.** reduce 20% corn at all HUC8 watersheds in the central U.S. Midwest.

export in streamflow.

Tile drainage changes the flow path of water and nitrogen, and further drives the spatial variation of nitrate exporting. Tile drainage facilitates shallow soil water draining (Danesh-Yazdi et al., 2016; Schilling et al., 2012), reduces water penetrating into deeper soil and the water storage in the shallow soil (Gramlich et al., 2018; Muma et al., 2016), which increases the quick flow and decreases slow flow. Besides, tile drainage reduces the nitrate residence time and further increases nitrate concentration in the stream (Table 1). Specifically, the spatial variation of tile drainage explains nearly a quarter of the spatial variation of C_{quick} in June. To the best of our knowledge, this study represents the first time that the impact of tile drainage on nitrate loading has been quantified at the regional scale. We also found a seasonality of the impact of tile drainage on water and nitrate exporting. Tile drainage plays a more important role during wet periods, as C_{quick} is significantly correlated with tile fraction ($p < 0.05$) for all months except during August (Fig. S18), and the Q_{95} is significantly correlated with tile fraction except for the dry months (from August to October) (Fig. S19). During dry months, low soil moisture caused by relatively lower precipitation and high crop water uptake limits the functioning of tile drainage to deliver water and nitrate (Lam et al., 2016).

4.3. *Future roadmap for modeling and monitoring agricultural nitrate export*

Nutrient loss reduction practices in the U.S. to date appear to be inadequate for meeting federal and state government goals (EPA, Illinois, 2021, EPA, 2015). This lack of progress may in part be attributed to the lack of incentives for growers to adopt certain management practices (EPA, Illinois, 2021), and inadequate geospatial targeting of such practices, both of which require improved scientific understanding to provide guidance. Our study provided a holistic view of how nitrogen cycles interact with hydrological cycles under heavily-managed agroecosystems. We found that the C~Q relationship in the U.S. Midwest cannot be characterized by a simple chemostatic or chemodynamic behavior. Instead, our finding largely confirms the "shallow and deep" hypothesis (Zhi and Li, 2020) that transitions from a quick-flow-dominated regime to a slow-flow-dominated regime are controlled by hydrological vertical mixing. Furthermore, we showed that shallow soil is directly controlled by both fast-responding hydrological inputs (e.g., rainfall, infiltration) and agricultural practices (e.g. corn fraction, fertilizer use), modulated by tile drainage. On the other hand, deep soil (including deep subsurface water and groundwater) has slower hydrological dynamics with low nitrate concentration (Botter

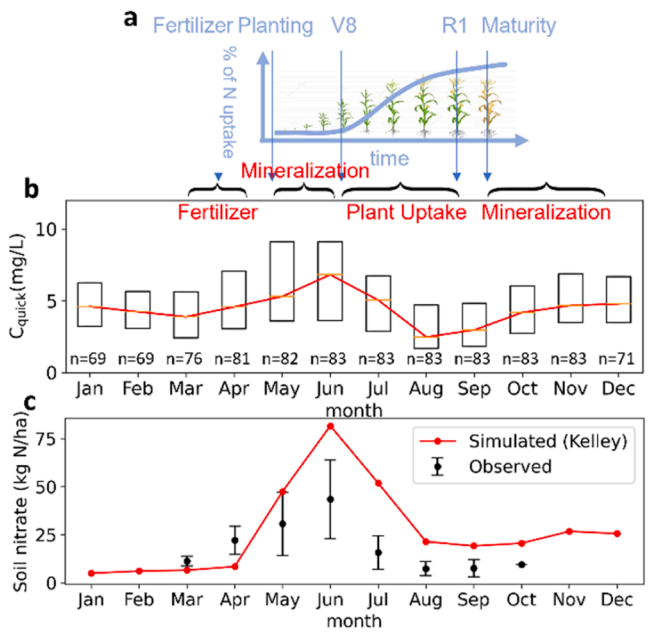

Fig. 11. Seasonal variation of C_{quick}. a. Schematic for uptake of nitrogen by corn. **b.** Boxplot of quick flow concentration (C_{quick}, estimated as the mean nitrate concentration between 90th percentile of discharge and 95th percentile discharge in a certain month) in different months in the observed watersheds (n: the number of watersheds with observed nitrate concentration). The middle, upper, and lower parts of the boxplots indicate 25%, 50%, and 75% quantile of the C_{quick}. **c.** Measurements of soil nitrate content in four fields in Kelley, IA and Nashua, IA in 2016 (Martinez-Feria et al., 2018). The error bar represents one standard deviation. The red line represents simulated soil nitrate content in a corn field at Kelley, IA in 2016 by an advanced agroecosystem model ecosys (Li et al., 2022).

et al., 2020; Ebeling et al., 2021). Our study developed a parsimonious process-based model to bring the above findings together mathematically, and this new model enabled us to quantitatively attribute the roles of agricultural practices and tile drainage in agricultural nitrate export and helped provide scenario assessments under different corn and tile drainage fractions. The findings reveal the fundamental coupling of hydrology and biogeochemistry from individual fields to watersheds to the region as a whole, which carries broad generality and applicability to different agriculture-dominant watersheds across the world.

Our study has generated a scientific and technological roadmap for modeling and monitoring agricultural nitrate export. First, the findings here can be further corroborated by in-situ measurements and monitoring networks. For example, stable isotope technology can be applied to measure nitrate from both shallow and deep soil layers to directly attribute the composition and sources of riverine nitrate (Hu et al., 2019). Second, cost-effective nitrate sensors deployable at stream gauges have the potential to build a monitoring network through the Internet-of-Things (IoT) technology, which could enable real-time monitoring and tracking of watershed-level nitrate dynamics (Saboe et al., 2021). Advanced remote sensing technologies enable the detection of management practices, such as crop rotation (Cai et al., 2018), plant nitrogen uptake (Wang et al., 2021), and cover crop adoption (Zhou et al., 2022), supporting on-the-ground tracking of the progress of desired practice adoption. The process-based agroecosystem models that can link field-to-watershed dynamics (Zhou et al., 2021), further empowered with artificial intelligence and the increasing amount of observations from diverse sources (Zhi et al., 2021), collectively should allow for customized designs for individual watersheds for prioritized changes in management practices on the ground to achieve the most effective nutrient loss reduction. The above scientific and technological roadmap will ultimately generate sufficient actionable insights that can enable both market-based incentive programs (e.g. water quality trading market) and optimized government policy-making, leading to real progress in nutrient loss reduction under a changing climate.

5. Conclusion

We analyzed historical stream nitrate and discharge data from 83 watersheds in the central U.S. Midwest and found a unique "two-stage" C~Q relationship over these agricultural watersheds. We further developed a hydrological vertical mixing model to explain the shape of the observed C~Q relationship at both the event and monthly scales and empirical parameterization schemes to predict nitrate concentrations, which were used to predict the C~Q relationship and nitrate load at all HUC8 watersheds in the central U.S. Midwest with daily stream discharge data from GRADES. The hydrological vertical mixing model suggests that the observed "two-stage" C~Q relationship in this region originates from the vertical mixing of quick flow with high nitrate levels from shallow soils and the slow flow with low nitrate levels from deeper soils. The hydrological vertical mixing model coupled with the seasonality of hydrology and agricultural practice explains the spatial and temporal variation of the C~Q relationship at the watershed scale. The planting of corn and installation of tile drainage has been found to change both the hydrological and biogeochemical processes and further controls the C~Q relationship. We found that the spatial variation of corn fraction and tile fraction explains 48.8% and 25.5% variation of C_{quick} in June, respectively. Our work reveals the underlying coupled hydrological and biogeochemical processes that shape the C~Q relationship and its spatial and temporal variation, and highlights the importance of managing tile drainage and fertilizer inputs in nutrient loss reduction. More broadly, our work provides a holistic framework for modeling and monitoring nitrate export over agricultural watersheds.

Declaration of Competing Interest

No

Data availability

All the data used in this research are publicly available online.

Acknowledgement

The authors acknowledge the financial support from NSF CAREER Award managed by NSF Environmental Sustainability Program (Award # 1847334), Illinois Nutrient Research & Education Council, the National Great Rivers Research and Education Center, Walton Family Foundation and USDA NIFA program.

Supplementary materials

Supplementary material associated with this article can be found, in the online version, at doi:10.1016/j.watres.2022.119468.

References

Alexander, R.B., Smith, R.A., Schwarz, G.E., Boyer, E.W., Nolan, J.V., Brakebill, J.W., 2008. Differences in phosphorus and nitrogen delivery to the Gulf of Mexico from the Mississippi River Basin. Environ. Sci. Technol. 42, 822–830.

Anders, A.M., Bettis, E.A., Grimley, D.A., Stumpf, A.J., Kumar, P., 2018. Impacts of quaternary history on critical zone structure and processes: examples and a conceptual model from the intensively managed landscapes critical zone observatory. Front. Earth Sci. Chin. 6 https://doi.org/10.3389/feart.2018.00024.

Andresen, Hilberg, 2012. Historical Climate and Climate Trends in the Midwestern USA. US National Climate.

Archontoulis, S.V., Castellano, M.J., Licht, M.A., Nichols, V., Baum, M., Huber, I., Martinez-Feria, R., Puntel, L., Ordóñez, R.A., Iqbal, J., Wright, E.E., Dietzel, R.N., Helmers, M., Vanloocke, A., Liebman, M., Hatfield, J.L., Herzmann, D., Carolina Córdova, S., Edmonds, P., Togliatti, K., Kessler, A., Danalatos, G., Pasley, H.,

Pederson, C., Lamkey, K.R., 2020. Predicting crop yields and soil-plant nitrogen dynamics in the US Corn Belt. Crop. Sci. https://doi.org/10.1002/csc2.20039.
Atkinson, L.A., Ross, M., Stumpf, A.J., 2014. Three-dimensional hydrofacies assemblages in ice-contact/proximal sediments forming a heterogeneous "hybrid" hydrostratigraphic unit in central Illinois, USA. Hydrogeol. J. 22, 1605–1624.
Baldwin, C.K., Lall, U., 1999. Seasonality of streamflow: the upper Mississippi river. Water Resour. Res. 35, 1143–1154.
Barbiero, R.P., Lesht, B.M., Hinchey, E.K., Nettesheim, T.G., 2018. A brief history of the U.S. EPA Great Lakes National Program Office's water quality survey. J. Great Lakes Res. 44, 539–546.
Basu, N.B., Destouni, G., Jawitz, J.W., Thompson, S.E., Loukinova, N.V., Darracq, A., Zanardo, S., Yaeger, M., Sivapalan, M., Rinaldo, A., Rao, P.S.C., 2010. Nutrient loads exported from managed catchments reveal emergent biogeochemical stationarity. Geophys. Res. Lett. 37 https://doi.org/10.1029/2010gl045168.
Basu, N.B., Jindal, P., Schilling, K.E., Wolter, C.F., Takle, E.S., 2012. Evaluation of analytical and numerical approaches for the estimation of groundwater travel time distribution. J. Hydrol. 475, 65–73.
Basu, N.B., Rao, P.S.C., Thompson, S.E., Loukinova, N.V., Donner, S.D., Ye, S., Sivapalan, M., 2011a. Spatiotemporal averaging of in-stream solute removal dynamics. Water Resour. Res. 47 https://doi.org/10.1029/2010wr010196.
Basu, N.B., Thompson, S.E., Rao, P.S.C., 2011b. Hydrologic and biogeochemical functioning of intensively managed catchments: a synthesis of top-down analyses. Water Resour. Res. 47 https://doi.org/10.1029/2011wr010800.
Bianchi, T.S., DiMarco, S.F., Cowan Jr., J.H., Hetland, R.D., Chapman, P., Day, J.W., Allison, M.A., 2010. The science of hypoxia in the Northern Gulf of Mexico: a review. Sci. Total Environ. 408, 1471–1484.
Bieroza, M.Z., Heathwaite, A.L., Bechmann, M., Kyllmar, K., Jordan, P., 2018. The concentration-discharge slope as a tool for water quality management. Sci. Total Environ. 630, 738–749.
Boesch, D.F., 2002. Challenges and opportunities for science in reducing nutrient over-enrichment of coastal ecosystems. Estuaries 25, 886–900.
Böhlke, J.K., Antweiler, R.C., Harvey, J.W., Laursen, A.E., Smith, L.K., Smith, R.L., Voytek, M.A., 2009. Multi-scale measurements and modeling of denitrification in streams with varying flow and nitrate concentration in the upper Mississippi River basin. USA. Biogeochem. 93, 117–141.
Botter, M., Li, L., Hartmann, J., Burlando, P., Fatichi, S., 2020. Depth of solute generation is a dominant control on concentration-discharge relations. Water Resour. Res. 56 https://doi.org/10.1029/2019wr026695.
Bowles, T.M., Atallah, S.S., Campbell, E.E., Gaudin, A.C.M., Wieder, W.R., Stuart Grandy, A., 2018. Addressing agricultural nitrogen losses in a changing climate. Nat. Sustainab. https://doi.org/10.1038/s41893-018-0106-0.
Cai, Y., Guan, K., Peng, J., Wang, S., Seifert, C., Wardlow, B., Li, Z., 2018. A high-performance and in-season classification system of field-level crop types using time-series Landsat data and a machine learning approach. Remote Sens. Environ. 210, 35–47.
Cao, P., Lu, C., Yu, Z., 2018. Historical nitrogen fertilizer use in agricultural ecosystems of the contiguous United States during 1850–2015: application rate, timing, and fertilizer types. Earth Syst. Sci. Data 10, 969–984.
Cheng, Y., Huang, M., Lawrence, D.M., Calvin, K., Lombardozzi, D.L., Sinha, E., Pan, M., He, X., 2022. Future bioenergy expansion could alter carbon sequestration potential and exacerbate water stress in the United States. Sci. Adv. 8, eabm8237.
Danesh-Yazdi, M., Foufoula-Georgiou, E., Karwan, D.L., Botter, G., 2016. Inferring changes in water cycle dynamics of intensively managed landscapes via the theory of time-variant travel time distributions. Water Resour. Res. 52, 7593–7614.
David, M.B., Drinkwater, L.E., McIsaac, G.F., 2010. Sources of nitrate yields in the Mississippi River Basin. J. Environ. Qual. 39, 1657–1667.
Donner, S.D., Kucharik, C.J., Foley, J.A., 2004. Impact of changing land use practices on nitrate export by the Mississippi River. Glob. Biogeochem. Cycles 18. https://doi.org/10.1029/2003gb002093.
Ebeling, P., Kumar, R., Weber, M., Knoll, L., Fleckenstein, J.H., Musolff, A., 2021. Archetypes and controls of riverine nutrient export across German catchments. Water Resour. Res. 57 https://doi.org/10.1029/2020wr028134.
EPA, Illinois, 2021. Illinois NLRS Biennial Report.
EPA, US., 2015. Mississippi River/Gulf of Mexico Watershed Nutrient Task Force 2015 Report to Congress: biennial Report 2015. United States Environmental Protection Agency.
U.S. Geological Survey, 2021, National Water Information System data available on the World Wide Web (USGS Water Data for the Nation), accessed 2021, at URL http://waterdata.usgs.gov/nwis/.
EPA, US., 2022. Hypoxia Task Force Nutrient Reduction Strategies. Retrieved from United States Environmental Protection Agency: https://www.epa.gov/ms-htf/hypoxia-task-force-nutrient-reduction-strategies.
Fenneman, F., Johnson, D.M., 1946. Physiographic divisions of the conterminous US United States Geological Survey.
FAO, 2022. FAO statistical databases. http://faostat.fao.org.
Fenneman, N., Johnson, D., 1946b. Physiographic Divisions of the Conterminous US Reston. US Geological Survey, VA.
Foley, J.A., Ramankutty, N., Brauman, K.A., Cassidy, E.S., Gerber, J.S., Johnston, M., Mueller, N.D., O'Connell, C., Ray, D.K., West, P.C., Balzer, C., Bennett, E.M., Carpenter, S.R., Hill, J., Monfreda, C., Polasky, S., Rockström, J., Sheehan, J., Siebert, S., Tilman, D., Zaks, D.P.M., 2011. Solutions for a cultivated planet. Nature 478, 337–342.
Galloway, J.N., Dentener, F.J., Capone, D.G., Boyer, E.W., Howarth, R.W., Seitzinger, S. P., Asner, G.P., Cleveland, C.C., Green, P.A., Holland, E.A., Karl, D.M., Michaels, A. F., Porter, J.H., Townsend, A.R., Vöosmarty, C.J., 2004. Nitrogen Cycles: Past, Present, and Future. Biogeochemistry 70, 153–226.
Godsey, S.E., Kirchner, J.W., Clow, D.W., 2009. Concentration-discharge relationships reflect chemostatic characteristics of US catchments. Hydrol. Process. 23, 1844–1864.
Gomez-Velez, J.D., Harvey, J.W., Cardenas, M.B., Kiel, B., 2015. Denitrification in the Mississippi River network controlled by flow through river bedforms. Nat. Geosci. 8, 941–945.
Gorski, G., Zimmer, M.A., 2021. Hydrologic regimes drive nitrate export behavior in human-impacted watersheds. Hydrol. Earth Syst. Sci. 25, 1333–1345.
Gramlich, A., Stoll, S., Stamm, C., Walter, T., Prasuhn, V., 2018. Effects of artificial land drainage on hydrology, nutrient and pesticide fluxes from agricultural fields–a review. Agric. Ecosyst. Environ. 266, 84–99.
Hahne, H.C.H., Kroontje, W., Lutz Jr, J.A., 1977. Nitrogen fertilization I. nitrate accumulation and losses under continuous corn cropping. Soil Sci. Soc. Am. J. 41, 562–567.
Hansen, A.T., Dolph, C.L., Foufoula-Georgiou, E., Finlay, J.C., 2018. Contribution of wetlands to nitrate removal at the watershed scale. Nat. Geosci. https://doi.org/10.1038/s41561-017-0056-6.
Harvey, J.W., Böhlke, J.K., Voytek, M.A., Scott, D., Tobias, C.R., 2013. Hyporheic zone denitrification: controls on effective reaction depth and contribution to whole-stream mass balance. Water Resour. Res. 49, 6298–6316.
Hirsch, R.M., De Cicco, L.A., 2015. User guide to Exploration and Graphics for RivEr Trends (EGRET) and dataRetrieval: R packages for hydrologic data. Techniq. Method. https://doi.org/10.3133/tm4a10.
Hirsch, R.M., Moyer, D.L., Archfield, S.A., 2010. Weighted regressions on time, discharge, and season (WRTDS), with an Application to Chesapeake Bay River Inputs. J. Am. Water Resour. Assoc. 46, 857–880.
Hooper, R.P., Christophersen, N., Peters, N.E., 1990. Modelling streamwater chemistry as a mixture of soilwater end-members — An application to the Panola Mountain catchment, Georgia, U.S.A. J. Hydrol. (Amst.). https://doi.org/10.1016/0022-1694(90)90131-g.
Howarth, R.W., Marino, R., 2006. Nitrogen as the limiting nutrient for eutrophication in coastal marine ecosystems: evolving views over three decades. Limnol. Oceanogr. 51, 364–376.
Hu, M., Liu, Y., Zhang, Y., Dahlgren, R.A., Chen, D., 2019. Coupling stable isotopes and water chemistry to assess the role of hydrological and biogeochemical processes on riverine nitrogen sources. Water Res. 150, 418–430.
Huston, M.A., 2005. The three phases of land-use change: implications for biodiversity. Ecol. Appl. 15, 1864–1878.
Inwood, S.E., Tank, J.L., Bernot, M.J., 2007. Factors controlling sediment denitrification in midwestern streams of varying land use. Microb. Ecol. 53, 247–258.
Kalita, P.K., Cooke, R.A.C., Anderson, S.M., Hirschi, M.C., Mitchell, J.K., 2007. Subsurface drainage and water quality: the Illinois experience. Transact. ASABE 50, 1651–1656.
King, K.W., Williams, M.R., Fausey, N.R., 2016. Effect of crop type and season on nutrient leaching to tile drainage under a corn–soybean rotation. J. Soil Water Conserv. 71, 56–68.
Koenig, L.E., Shattuck, M.D., Snyder, L.E., Potter, J.D., McDowell, W.H., 2017. Deconstructing the effects of flow on DOC, nitrate, and major ion interactions using a high-frequency aquatic sensor network. Water Resour. Res. 53, 10655–10673.
Kohl, D.H., Shearer, G.B., Commoner, B., 1971. Fertilizer nitrogen: contribution to nitrate in surface water in a corn belt watershed. Science 174, 1331–1334.
Lam, W.V., Macrae, M.L., English, M.C., O'Halloran, I.P., Plach, J.M., Wang, Y., 2016. Seasonal and event-based drivers of runoff and phosphorus export through agricultural tile drains under sandy loam soil in a cool temperate region. Hydrol. Process. 30, 2644–2656.
Laurent, A., Fennel, K., 2019. Time-evolving, spatially explicit forecasts of the Northern Gulf of Mexico Hypoxic Zone. Environ. Sci. Technol. 53, 14449–14458.
Lee, E.S., Krothe, N.C., 2001. A four-component mixing model for water in a karst terrain in south-central Indiana, USA. Using solute concentration and stable isotopes as tracers. Chem. Geol. 179, 129–143.
Lin, P., Pan, M., Beck, H.E., Yang, Y., Yamazaki, D., Frasson, R., David, C.H., Durand, M., Pavelsky, T.M., Allen, G.H., Gleason, C.J., Wood, E.F., 2019. Global reconstruction of naturalized river flows at 2.94 million reaches. Water Resour. Res. 55, 6499–6516.
Liu, C., Sun, G., McNulty, S.G., Noormets, A., Fang, Y., 2016. Environmental controls on seasonal ecosystem evapotranspiration/potential evapotranspiration ratio as determined by the global eddy flux measurements. Hydrol. Earth Syst. Sci. 21, 311–322.
Li, Z., Guan, K., Zhou, W., Peng, B., Jin, Z., Tang, J., Grant, R.F., Nafziger, E., Margenot, A.J., Gentry, L.E., DeLucia, E.H., Yang, W.H., Cai, Y., Qin, Z., Archontoulis, S., Fernández, F.G., Yu, Z., Do Kyoung, L., Yang, Y., 2022. Assessing the impacts of pre-growing-season weather conditions on soil nitrogen dynamics and corn productivity in the U.S. Midwest. Field Crop. Res.
Loftin, K.A., Graham, J.L., Hilborn, E.D., Lehmann, S.C., Meyer, M.T., Dietze, J.E., Griffith, C.B., 2016. Cyanotoxins in inland lakes of the United States: occurrence and potential recreational health risks in the EPA National Lakes Assessment 2007. Harm. Algae 56, 77–90.
Lyne, V., Hollick, M., 1979. Stochastic Time-Variable Rainfall-Runoff Modelling. Institute of Engineers Australia National Conference. Institute of Engineers Australia Barton, Australia, pp. 89–93.
Marinos, R.E., Van Meter, K.J., Basu, N.B., 2020. Is the river a chemostat?: Scale versus land use controls on nitrate concentration-discharge dynamics in the upper Mississippi river basin. Geophys. Res. Lett. 47 e2020GL087051.
Martinez-Feria, R.A., Castellano, M.J., Dietzel, R.N., Helmers, M.J., Liebman, M., Huber, I., Archontoulis, S.V., 2018. Linking crop- and soil-based approaches to evaluate system nitrogen-use efficiency and tradeoffs. Agricult. Ecosyst. Environ. https://doi.org/10.1016/j.agee.2018.01.002.

Minaudo, C., Dupas, R., Gascuel-Odoux, C., Roubeix, V., Danis, P.-A., Moatar, F., 2019. Seasonal and event-based concentration-discharge relationships to identify catchment controls on nutrient export regimes. Adv. Water Resour. 131, 103379.
Mishra, V., Cherkauer, K.A., Niyogi, D., Lei, M., Pijanowski, B.C., Ray, D.K., Bowling, L. C., Yang, G., 2010. A regional scale assessment of land use/land cover and climatic changes on water and energy cycle in the upper Midwest United States. Int. J. Climatol. 30, 2025–2044.
Moatar, F., Abbott, B.W., Minaudo, C., Curie, F., Pinay, G., 2017. Elemental properties, hydrology, and biology interact to shape concentration-discharge curves for carbon, nutrients, sediment, and major ions. Water Resour. Res. 53, 1270–1287.
Mulholland, P.J., Helton, A.M., Poole, G.C., Hall, R.O., Hamilton, S.K., Peterson, B.J., Tank, J.L., Ashkenas, L.R., Cooper, L.W., Dahm, C.N., Dodds, W.K., Findlay, S.E.G., Gregory, S.V., Grimm, N.B., Johnson, S.L., McDowell, W.H., Meyer, J.L., Valett, H. M., Webster, J.R., Arango, C.P., Beaulieu, J.J., Bernot, M.J., Burgin, A.J., Crenshaw, C.L., Johnson, L.T., Niederlehner, B.R., O'Brien, J.M., Potter, J.D., Sheibley, R.W., Sobota, D.J., Thomas, S.M., 2008. Stream denitrification across biomes and its response to anthropogenic nitrate loading. Nature 452, 202–205.
Muma, M., Rousseau, A.N., Gumiere, S.J., 2016. Assessment of the impact of subsurface agricultural drainage on soil water storage and flows of a small watershed. Water (Basel) 8, 326.
Musolff, A., Schmidt, C., Selle, B., Fleckenstein, J.H., 2015. Catchment controls on solute export. Adv. Water Resour. 86, 133–146.
Musolff, A., Zhan, Q., Dupas, R., Minaudo, C., Fleckenstein, J.H., Rode, M., Dehaspe, J., Rinke, K., 2021. Spatial and temporal variability in concentration-discharge relationships at the event scale. Water Resour. Res. 57 https://doi.org/10.1029/2020wr029442.
Nakagaki, N., Wieczorek, M.E., 2016. Estimates of subsurface tile drainage extent for 12 Midwest states, 2012. US Geolog. Surv. Data Release. https://doi.org/10.5066/F7W37TDP.
NASS, U.S.D.A., 2019a. 2017 Census of Agriculture: United States Summary and State Data. Volume 1. Geograph. Area Ser.
NASS, USDA., 2019b. 2018 Agricultural Chemical Use Survey. USDA National Agricultural Statistics Service.
NLRS, 2021. Process for updating existing practices or adding new practices to the Illinois Nutrient Loss Reduction Strategy. Retrieved from Illinois Environmental Protection Agency: https://www2.illinois.gov/epa/topics/water-quality/watershed-management/excess-nutrients/Documents/NLRS-Practice-Approval_Process_Updated_202104.pdf.
NASS, USDA., 2021. USDA national agricultural statistics service cropland data layer. Publ. Crop. data layer. https://nassgeodata.gmu.edu/CropScape/. accessed 5. 18. 16.
Pachauri, R.K., Allen, M.R., Barros, V.R., Broome, J., Cramer, W., Christ, R., Church, J.A., Clarke, L., Dahe, Q., Dasgupta, P., Dubash, N.K., Edenhofer, O., Elgizouli, I., Field, C. B., Forster, P., Friedlingstein, P., Fuglestvedt, J., Gomez-Echeverri, L., Hallegatte, S., Hegerl, G., Howden, M., Jiang, K., Jimenez Cisneroz, B., Kattsov, V., Lee, H., Mach, K.J., Marotzke, J., Mastrandrea, M.D., Meyer, L., Minx, J., Mulugetta, Y., O'Brien, K., Oppenheimer, M., Pereira, J.J., Pichs-Madruga, R., Plattner, G.-K., Pörtner, H.-O., Power, S.B., Preston, B., Ravindranath, N.H., Reisinger, A., Riahi, K., Rusticucci, M., Scholes, R., Seyboth, K., Sokona, Y., Stavins, R., Stocker, T.F., Tschakert, P., van Vuuren, D., van Ypserle, J.-P., 2014. Climate Change 2014: Synthesis Report. Contribution of Working Groups I, II and III to the Fifth Assessment Report of the Intergovernmental Panel On Climate Change. IPCC, Geneva, Switzerland.
Pinay, G., Black, V.J., Planty-Tabacchi, A.M., Gumiero, B., Décamps, H., 2000. Geomorphic control of denitrification in large river floodplain soils. Biogeochemistry 50, 163–182.
Pohle, I., Baggaley, N., Palarea-Albaladejo, J., Stutter, M., Glendell, M., 2021. A framework for assessing concentration-discharge catchment behavior from low-frequency water quality data. Water Resour. Res. 57 https://doi.org/10.1029/2021wr029692.
Quan, Z., Zhang, X., Davidson, E.A., Zhu, F., Li, S., Zhao, X., Chen, X., Zhang, L., He, J., Wei, W., Fang, Y., 2021. Fates and use efficiency of nitrogen fertilizer in maize cropping systems and their responses to technologies and management practices: a global analysis on field 15 N tracer studies. Earth's Future. https://doi.org/10.1029/2020ef001514.
Rabalais, N.N., Turner, R.E., Scavia, D., 2002. Beyond Science into Policy: Gulf of Mexico Hypoxia and the Mississippi River: nutrient policy development for the Mississippi River watershed reflects the accumulated scientific evidence that the increase in nitrogen loading is the primary factor in the worsening of hypoxia in the northern Gulf of Mexico. Bioscience 52, 129–142.
Robertson, D.M., Saad, D.A., 2021. Nitrogen and phosphorus sources and delivery from the Mississippi/Atchafalaya river basin: an update using 2012 SPARROW models. J. Am. Water Resour. Assoc. 57, 406–429.
Saboe, D., Ghasemi, H., Gao, M.M., Samardzic, M., Hristovski, K.D., Boscovic, D., Burge, S.R., Burge, R.G., Hoffman, D.A., 2021. Real-time monitoring and prediction of water quality parameters and algae concentrations using microbial potentiometric sensor signals and machine learning tools. Sci. Total Environ. https://doi.org/10.1016/j.scitotenv.2020.142876.
Saiers, J.E., Fair, J.H., Shanley, J.B., Hosen, J., Matt, S., Ryan, K.A., Raymond, P.A., 2021. Evaluating streamwater dissolved organic carbon dynamics in context of variable flowpath contributions with a tracer-based mixing model. Water Resour. Res. 57 https://doi.org/10.1029/2021wr030529.
Schilling, K.E., Jindal, P., Basu, N.B., Helmers, M.J., 2012. Impact of artificial subsurface drainage on groundwater travel times and baseflow discharge in an agricultural watershed, Iowa (USA). Hydrol. Process. 26, 3092–3100.
Schilling, K.E., Wolter, C.F., Isenhart, T.M., Schultz, R.C., 2015. Tile drainage density reduces groundwater travel times and compromises Riparian buffer effectiveness. J. Environ. Qual. 44, 1754–1763.
Sears, P.B., 1926. The natural vegetation op Ohio II. The prairies.
Shanley, J.B., McDowell, W.H., Stallard, R.F., 2011. Long-term patterns and short-term dynamics of stream solutes and suspended sediment in a rapidly weathering tropical watershed. Water Resour. Res. 47.
Sinha, E., Michalak, A.M., Calvin, K.V., Lawrence, P.J., 2019. Societal decisions about climate mitigation will have dramatic impacts on eutrophication in the 21st century. Nat. Commun. https://doi.org/10.1038/s41467-019-08884-w.
Soller, D.R., Reheis, M.C., Garrity, C.P., Van Sistine, D.R., 2009. Map database for surficial materials in the conterminous United States. US Geolog. Surv. Data Ser. 425.
Stewart, B., Shanley, J.B., Kirchner, J.W., Norris, D., Adler, T., Bristol, C., Harpold, A.A., Perdrial, J.N., Rizzo, D.M., Sterle, G., Underwood, K.L., Wen, H., Li, L., 2022. Streams as mirrors: Reading subsurface water chemistry from stream chemistry. Water Resour. Res. 58. https://doi.org/10.1029/2021wr029931.
Thomas, Z., Abbott, B.W., Troccaz, O., Baudry, J., Pinay, G., 2016. Proximate and ultimate controls on carbon and nutrient dynamics of small agricultural catchments. Biogeosciences. https://doi.org/10.5194/bg-13-1863-2016.
Thompson, S.E., Basu, N.B., Lascurain, J., 2011. Relative dominance of hydrologic versus biogeochemical factors on solute export across impact gradients. Water Resour.
Turner, R.E., Rabalais, N.N., 1994. Coastal eutrophication near the Mississippi river delta. Nature 368, 619–621.
Van Meter, K.J., Basu, N.B., Veenstra, J.J., Burras, C.L., 2016. The nitrogen legacy: emerging evidence of nitrogen accumulation in anthropogenic landscapes. Environ. Res. Lett. https://doi.org/10.1088/1748-9326/11/3/035014.
Wang, S., Guan, K., Wang, Z., Ainsworth, E.A., Zheng, T., Townsend, P.A., Liu, N., Nafziger, E., Masters, M.D., Li, K., Wu, G., Jiang, C., 2021. Airborne hyperspectral imaging of nitrogen deficiency on crop traits and yield of maize by machine learning and radiative transfer modeling. Int. J. Appl. Earth Obs. Geoinf. 105, 102617.
Westra, S., Fowler, H.J., Evans, J.P., Alexander, L.V., Berg, P., Johnson, F., Kendon, E.J., Lenderink, G., Roberts, N.M., 2014. Future changes to the intensity and frequency of short-duration extreme rainfall. Rev. Geophys. 52, 522–555.
Winter, C., Tarasova, L., Lutz, S.R., Musolff, A., Kumar, R., Fleckenstein, J.H., 2022. Explaining the variability in high-frequency nitrate export patterns using long-term hydrological event classification. Water Resour. Res. 58 https://doi.org/10.1029/2021wr030938.
Wollheim, W.M., Bernal, S., Burns, D.A., Czuba, J.A., Driscoll, C.T., Hansen, A.T., Hensley, R.T., Hosen, J.D., Inamdar, S., Kaushal, S.S., Koenig, L.E., Lu, Y.H., Marzadri, A., Raymond, P.A., Scott, D., Stewart, R.J., Vidon, P.G., Wohl, E., 2018. River network saturation concept: factors influencing the balance of biogeochemical supply and demand of river networks. Biogeochemistry 141, 503–521.
Yang, Y., Pan, M., Beck, H.E., Fisher, C.K., Beighley, R.E., Kao, S.-C., Hong, Y., Wood, E. F., 2019. In quest of calibration density and consistency in hydrologic modeling: distributed parameter calibration against streamflow characteristics. Water Resour. Res. 55, 7784–7803.
Zhang, X., Davidson, E.A., Mauzerall, D.L., Searchinger, T.D., Dumas, P., Shen, Y., 2015. Managing nitrogen for sustainable development. Nature 528, 51–59.
Zhi, W., Feng, D., Tsai, W.-.P., Sterle, G., Harpold, A., Shen, C., Li, L., 2021. From Hydrometeorology to River Water Quality: can a Deep Learning Model Predict Dissolved Oxygen at the Continental Scale? Environ. Sci. Technol. 55, 2357–2368.
Zhi, W., Li, L., 2020. The shallow and deep hypothesis: subsurface vertical chemical contrasts shape nitrate export patterns from different land uses. Environ. Sci. Technol. https://doi.org/10.1021/acs.est.0c01340.
Zhou, Q., Guan, K., Wang, S., Jiang, C., Huang, Y., Peng, B., Chen, Z., Wang, S., Hipple, J., Sheafer, D., 2022. Recent rapid increase of cover crop adoption across the US Midwest detected by fusing multi-source satellite data. EarthArXiv. https://doi.org/10.31223/X5JW70.
Zhou, W., Guan, K., Peng, B., Tang, J., Jin, Z., Jiang, C., Grant, R., Mezbahuddin, S., 2021. Quantifying carbon budget, crop yields and their responses to environmental variability using the ecosys model for U.S. Midwestern agroecosystems. Agric. For. Meteorol. 307, 108521.